Palmitic acid induces neurotoxicity and gliatoxicity in SH-SY5Y human neuroblastoma and T98G human glioblastoma cells (#25280)

First submission

Editor guidance

Please submit by **16 Mar 2018** for the benefit of the authors (and your $200 publishing discount).

Structure and Criteria
Please read the 'Structure and Criteria' page for general guidance.

Custom checks
Make sure you include the custom checks shown below, in your review.

Raw data check
Review the raw data. Download from the location described by the author.

Image check
Check that figures and images have not been inappropriately manipulated.

Privacy reminder: If uploading an annotated PDF, remove identifiable information to remain anonymous.

Files

Download and review all files from the materials page.

5 Figure file(s)

Custom checks

Cell line checks

Is the correct provenance of the cell line described?

Structure and Criteria

Structure your review

The review form is divided into 5 sections.
Please consider these when composing your review:

1. **BASIC REPORTING**
2. **EXPERIMENTAL DESIGN**
3. **VALIDITY OF THE FINDINGS**
4. General comments
5. Confidential notes to the editor

You can also annotate this PDF and upload it as part of your review

When ready submit online.

Editorial Criteria

Use these criteria points to structure your review. The full detailed editorial criteria is on your guidance page.

BASIC REPORTING

- Clear, unambiguous, professional English language used throughout.
- Intro & background to show context. Literature well referenced & relevant.
- Structure conforms to PeerJ standards, discipline norm, or improved for clarity.
- Figures are relevant, high quality, well labelled & described.
- Raw data supplied (see PeerJ policy).

EXPERIMENTAL DESIGN

- Original primary research within Scope of the journal.
- Research question well defined, relevant & meaningful. It is stated how the research fills an identified knowledge gap.
- Rigorous investigation performed to a high technical & ethical standard.
- Methods described with sufficient detail & information to replicate.

VALIDITY OF THE FINDINGS

- Impact and novelty not assessed. Negative/inconclusive results accepted. *Meaningful* replication encouraged where rationale & benefit to literature is clearly stated.
- Data is robust, statistically sound, & controlled.
- Conclusions are well stated, linked to original research question & limited to supporting results.
- Speculation is welcome, but should be identified as such.

Standout reviewing tips

The best reviewers use these techniques

Tip	*Example*
Support criticisms with evidence from the text or from other sources	*Smith et al (J of Methodology, 2005, V3, pp 123) have shown that the analysis you use in Lines 241-250 is not the most appropriate for this situation. Please explain why you used this method.*
Give specific suggestions on how to improve the manuscript	*Your introduction needs more detail. I suggest that you improve the description at lines 57- 86 to provide more justification for your study (specifically, you should expand upon the knowledge gap being filled).*
Comment on language and grammar issues	*The English language should be improved to ensure that an international audience can clearly understand your text. Some examples where the language could be improved include lines 23, 77, 121, 128 – the current phrasing makes comprehension difficult.*
Organize by importance of the issues, and number your points	*1. Your most important issue* *2. The next most important item* *3. …* *4. The least important points*
Please provide constructive criticism, and avoid personal opinions	*I thank you for providing the raw data, however your supplemental files need more descriptive metadata identifiers to be useful to future readers. Although your results are compelling, the data analysis should be improved in the following ways: AA, BB, CC*
Comment on strengths (as well as weaknesses) of the manuscript	*I commend the authors for their extensive data set, compiled over many years of detailed fieldwork. In addition, the manuscript is clearly written in professional, unambiguous language. If there is a weakness, it is in the statistical analysis (as I have noted above) which should be improved upon before Acceptance.*

Palmitic acid induces neurotoxicity and gliatoxicity in SH-SY5Y human neuroblastoma and T98G human glioblastoma cells

Yee-Wen Ng [1] , **Yee-How Say** Corresp. [1]

[1] Department of Biomedical Science, Faculty of Science, Universiti Tunku Abdul Rahman (UTAR) Kampar Campus, Kampar, Perak, Malaysia

Corresponding Author: Yee-How Say
Email address: sayyh@utar.edu.my

Background. Obesity-related CNS pathologies like neuroinflammation and reactive gliosis are associated with high-fat diet (HFD) related elevation of saturated fatty acids like palmitic acid (PA) in neurons and astrocytes of the brain.

Methods. Human neuroblastoma cells SH-SY5Y (as a neuronal model), stably-transfected and human glioblastoma cells T98G (as an astrocytic model), were treated with 100-500 µM palmitic acid (PA), oleic acid (OA) or lauric acid (LA) for 24 h or 48 h, and their cell viability was assessed by 3-(4,5-dimetylthiazol-2-yl)-2,5-diphenyltetrazolium bromide (MTT) assay. The effects of stable overexpression of γ-synuclein (γ-syn), a neuronal protein recently recognized as a novel regulator of lipid handling in adipocytes, and transient overexpression of Parkinson's disease (PD) α-synuclein [α-syn; wild-type (wt) and its pathogenic mutants A53T, A30P and E46K] in SH-SY5Y and T98G cells, were also evaluated. The effects of co-treatment of PA with paraquat (PQ), a Parkinsonian pesticide, and leptin, a hormone involved in the brain-adipose axis, were also assessed. Intracellular lipid droplet accumulation was assessed by Oil Red O (ORO) staining. Cell death mode and cell cycle were analyzed by Annexin V/PI and PI flow cytometry. Reactive oxygen species (ROS) level was determined using 2',7'-dichlorofluorescien diacetate (DCFH-DA) assay and lipid peroxidation level was determined using thiobarbituric acid reactive substances (TBARS) assay.

Results. MTT assay revealed dose- and time-dependent PA cytotoxicity on SH-SY5Y and T98G cells, but not OA and LA. The cytotoxicity was significantly lower in SH-SY5Y-γ-syn cells, while transient overexpression of wt α-syn or its PD mutants (A30P and E46K, but not A53T) modestly (but still significantly) rescued the neurotoxicity of PA in SH-SY5Y and T98G cells. The cytotoxicity of PA correlates with increased ORO staining in SH-SY5Y and T98G cells treated with PA. Co-treatment of increasing concentrations of PQ exacerbated PA's neurotoxicity. Pre-treatment of leptin, a cytoprotective adipokine, did not protect SH-SY5Y cells from PA-induced cytotoxicity - suggesting a mechanism of PA-induced leptin resistance. Annexin V/PI flow cytometry analysis revealed PA-induced increase in percentages of cells in annexin V-positive/PI-negative quadrant (early apoptosis) and subG_0-G_1 fraction, accompanied by a decrease in G_2-M phase cells. The PA-induced ROS production and lipid peroxidation was at greater extent in T98G as compared to that in SH-SY5Y.

Discussion. In conclusion, PA induces apoptosis by increasing oxidative stress in neurons and astrocytes. Taken together, the results suggest that HFD may cause neuronal and astrocytic damage, which indirectly proposes that CNS pathologies involving neuroinflammation and reactive gliosis could be prevented via the diet regimen.

Palmitic acid induces neurotoxicity and gliatoxicity in SH-SY5Y human neuroblastoma and T98G human glioblastoma cells

Yee-Wen Ng[1], Yee-How Say[1]

[1]Department of Biomedical Science, Faculty of Science, Universiti Tunku Abdul Rahman (UTAR) Kampar Campus, Kampar, Perak, Malaysia.

*Corresponding author:

Yee-How Say[1]

Email address: sayyh@utar.edu.my

Abstract

Background. Obesity-related CNS pathologies like neuroinflammation and reactive gliosis are associated with high-fat diet (HFD) related elevation of saturated fatty acids like palmitic acid (PA) in neurons and astrocytes of the brain.

Methods. Human neuroblastoma cells SH-SY5Y (as a neuronal model), stably-transfected and human glioblastoma cells T98G (as an astrocytic model), were treated with 100-500 μM palmitic acid (PA), oleic acid (OA) or lauric acid (LA) for 24 h or 48 h, and their cell viability was assessed by 3-(4,5-dimetylthiazol-2-yl)-2,5-diphenyltetrazolium bromide (MTT) assay. The effects of stable overexpression of γ-synuclein (γ-syn), a neuronal protein recently recognized as a novel regulator of lipid handling in adipocytes, and transient overexpression of Parkinson's disease (PD) α-synuclein [α-syn; wild-type (wt) and its pathogenic mutants A53T, A30P and E46K] in SH-SY5Y and T98G cells, were also evaluated. The effects of co-treatment of PA with paraquat (PQ), a Parkinsonian pesticide, and leptin, a hormone involved in the brain-adipose axis, were also assessed. Intracellular lipid droplet accumulation was assessed by Oil Red O (ORO) staining. Cell death mode and cell cycle were analyzed by Annexin V/PI and PI flow cytometry. Reactive oxygen species (ROS) level was determined using 2',7'-dichlorofluorescien diacetate (DCFH-DA) assay and lipid peroxidation level was determined using thiobarbituric acid reactive substances (TBARS) assay.

Results. MTT assay revealed dose- and time-dependent PA cytotoxicity on SH-SY5Y and T98G cells, but not OA and LA. The cytotoxicity was significantly lower in SH-SY5Y-γ-syn cells, while transient overexpression of wt α-syn or its PD mutants (A30P and E46K, but not A53T)

modestly (but still significantly) rescued the neurotoxicity of PA in SH-SY5Y and T98G cells. The cytotoxicity of PA correlates with increased ORO staining in SH-SY5Y and T98G cells treated with PA. Co-treatment of increasing concentrations of PQ exacerbated PA's neurotoxicity. Pre-treatment of leptin, a cytoprotective adipokine, did not protect SH-SY5Y cells from PA-induced cytotoxicity - suggesting a mechanism of PA-induced leptin resistance. Annexin V/PI flow cytometry analysis revealed PA-induced increase in percentages of cells in annexin V-positive/PI-negative quadrant (early apoptosis) and subG_0-G_1 fraction, accompanied by a decrease in G_2-M phase cells. The PA-induced ROS production and lipid peroxidation was at greater extent in T98G as compared to that in SH-SY5Y.

Discussion. In conclusion, PA induces apoptosis by increasing oxidative stress in neurons and astrocytes. Taken together, the results suggest that HFD may cause neuronal and astrocytic damage, which indirectly proposes that CNS pathologies involving neuroinflammation and reactive gliosis could be prevented via the diet regimen.

1. Introduction

Obesity is now a global health issue that presents a major risk for serious diet-related noncommunicable diseases including diabetes mellitus, cardiovascular diseases, hypertension, stroke, and some cancers (World Health Organization, 2017). High-fat diet (HFD) rich in saturated fatty acids (SFAs) has long been recognised to contribute to many adverse metabolic health issues. In the past two decades, it was found that HFD-induced obesity has been associated with neuroinflammation and reactive gliosis (Dorfman & Thaler, 2015), leading to CNS pathologies such as neurodegenerative diseases (Guillemot-Legris and Muccioli, 2017). A case-control study demonstrated a link between the intake of fat from animal sources rich in SFA and Parkinson's disease (PD) (Logroscino et al., 1996). Several prospective studies also showed association of BMI with increased risk of Alzheimer's disease (AD) (Gustafson et al., 2003) and Parkinson's disease (PD) (Hu et al., 2006); and on the contrary, lower BMI is associated with lower risk of PD (Sääksjärvi et al., 2014). Furthermore, the first study in humans using positron emission tomography with [^{11}C]-palmitate and [^{18}F]fluoro-6-thia-heptadecanoic acid ([^{18}F]-FTHA) showed increased fatty acid (FA) uptake and accumulation in the brain of obese subjects with metabolic syndrome (Karmi et al., 2010). This suggests that FAs are able to cross the blood-brain-barrier (BBB) and are able to be taken up by brain cells. In fact, peripheral FAs were

shown to have relationship with central FAs, as reported by a study done on human whole blood and cerebrospinal fluid (Guest et al., 2013).

Palmitic acid (PA), a long chain 16:0 SFA, is the most common fatty acid found in animals and plants such as palm oil, palm kernel oil, butter, cheese, milk and meat (Gunstone et al., 2010). Despite its crucial biological functions such as energy storage, acting as a signalling molecule and maintaining integrity of cellular membranes (Gunstone et al., 2010), PA has been found to be increased in diseased brains. Particularly, PA level appeared to be increased in the frontal cortex lipid rafts in PD (Fabelo et al., 2011); and in parietal cortex in AD (Fraser et al., 2010). Furthermore, PA was found to cause lipotoxicity to several cell lines *in vitro*. For instance, PA triggered the release of tumour necrosis factor-α (TNF-α) and interleukin-6 (IL-6), activating inflammatory signalling in astrocytes (Gupta et al., 2012). PA also induced apoptosis in human hepatoma cell line, HepG2 (Zhang et al., 2004), neural progenitor cells (Park et al., 2011) and neuronal cell line, SH-SY5Y (Hsiao et al., 2014).

Other than neurons, the brain also comprises and depends on surrounding non-neuronal cells such as glial, epithelial cells, pericytes and endothelia, for them to function correctly (Freire-Regatillo et al., 2017). Glial cells were once thought of to be only supportive systems for neurons. Now they are found to possess modulatory, trophic and immune functions in the brain (Gupta et al., 2012). Astrocyte is a type of glial cell, which is the most plentiful and varied non-neuronal cell in the CNS (Argente-arizón et al., 2015). Of note, marked astrogliosis was observed in the hypothalamus of HFD-induced or genetically obese mice (Buckman et al., 2013), suggesting that astrocyte plays a role in reactive gliosis leading to CNS pathologies.

A family of neuronal proteins that are implicated in both obesity and CN pathologies is the synucleins, i.e., α- and γ-synucleins (α-syn, γ-syn). They are small, soluble, highly conserved proteins, predominantly expressed in the neurons. α-syn is a major component of Lewy bodies and Lewy neurites appearing in the postmortem brain of PD and other synucleinopathies (Spillantini & Goedert, 2000). Genetic mutations in α-syn, including point mutations (A53T, A30P and E46K), have been linked to familial PD (Polymeropoulos et al., 1997). Neuronal expression of either human wild-type (wt) or PD-related mutant α-syn induces neurodegeneration associated with pathological accumulations of α-syn. Previous studies also revealed that α-syn-containing inclusion bodies were present in astrocytes of sporadic PD (Wakabayashi et al., 2000; Braak et al., 2007) and over-expression of wt α-syn in U373 astrocytoma cells induces of astroglial apoptotic cell death (Stefanova et al., 2001). Moreover α-syn and γ-syn were found to affect lipid uptake and metabolism in brain and adipocytes (Golovko et al., 2005; Millership et al., 2013; Hsiao et al., 2017).

Given the involvement of FAs particularly PA in CNS pathologies and the possible role of α-syn and γ-syn in modulating the effects of FAs, therefore, the objective of this study were first to evaluate the effects of PA, oleic acid (OA; long chain FA with lipid number of C18:1 *cis-9* and a major constituent in plant oil such as olive oil, almond oil, pecan oil and canola oil) and lauric acid (LA; medium chain 12:0 SFA which comprises about 50 % of fatty acid content in coconut oil, coconut milk, laurel oil and palm kernel oil) on the viability of human neuroblastoma SH-SY5Y and human glioblastoma T98G cell lines. SH-SY5Y cells were selected for the experiments as they have been widely used as a cell model of dopaminergic neurons for PD

research (Xie et al., 2010), while T98G cells were selected due to its biological resemblance with primary astrocytes and its broad use in research as an astrocyte cell model (Avila Rodriguez et al. 2014; Cabezas et al. 2015; Avila-Rodriguez et al. 2016). The effects of stable overexpression of γ-syn in SH-SY5Y and transient overexpression of α-syn (wt and PD mutants A53T, A30P and E46K) in SH-SY5Y and T98G cells were also evaluated. We found that PA is neurotoxic and gliatoxic to SH-SY5Y and T98G cells, respectively. To investigate the potential synergistic effect of environmental factors for dopaminergic neurotoxicity, SH-SY5Y cells were co-treated with the PA (to mimic HFD exposure), and increasing concentrations of paraquat (PQ), a herbicide that is implicated in the development of PD (Pezzoli and Cereda, 2013). Since leptin, a hormone that is involved in the brain-adipose axis, has been shown to have neuroprotective effect in SH-SY5Y cells (Russo et al., 2004; Lu et al., 2006; Weng et al., 2007), we also investigated whether leptin pre-treatment could rescue SH-SY5Y cells from PA neurotoxicity. Lastly, the mode of cell death induction by PA in SH-SY5Y and T98G was investigated using Annexin V/PI flow cytometry, and to attribute whether apoptotic cell death is caused by oxidative stress, intracellular reactive oxygen species (ROS) and extent of lipid peroxidation (Thiobarbituric Acid Reactive Substances - TBARS level) were assessed.

2. Materials and methods

2.1 Cell culture and treatments

SH-SY5Y (ATCC® CRL-2266™) and T98G (ATCC® CRL-1690™), obtained from the American Type Culture Collection (ATCC), were maintained in Eagle's Minimum Essential Medium (EMEM) (Corning, NY, USA) and Dulbecco's Modified Eagle's Medium (DMEM) (Corning, NY, USA), respectively, supplemented with 10% (v/v) fetal bovine serum (Sigma-

Aldrich, MO, USA) and 1% (v/v) penicillin–streptomycin (Nacalai Tesque, Japan) at 37°C and 5% CO_2 in air. All cell lines have been checked to ensure they are free of contamination and have been used from young stock (less than 7 passages). SH-SY5Y overexpressing γ-Syn SH-SY5Y-γ) was established by stably transfecting the SH-SY5Y cells with plasmid pOTB7 with full length human γ-syn (accession number: BC014098) cDNA (clone ID: 4546444; obtained from Addgene, MA, USA). Transfection was performed by electroporation using ECM® 830 ElectroSquarePorator™ (BTX Harvard Apparatus, Holliston, MA) and cells were cultured in complete growth medium for 72 h prior to 14 days of antibiotic selection with 1 mg/ml of G418 sulfate (A.G. Scientific Inc., USA). γ-synuclein protein expression after establishment of stable cells was assessed by Western blot using anti-γ-synuclein primary antibody, clone EP1539Y (Millipore, USA) prepared in 1: 5000 dilution and secondary HRP-conjugated anti-rabbit IgG antibody (Sigma Aldrich, USA) prepared in 1:10000 dilution (data not shown).

The FA-bovine serum albumin (FA-BSA) complex was prepared according to Hsiao et al., (2014) with slight modification. Briefly, 20 mM of FA was prepared in 0.01 N sodium hydroxide in a dry bath of 80 °C. MEM or DMEM with 1% BSA was added to different volumes of FA stock solution to reach final concentrations of 100 to 500 µM. The mixtures were incubated in the 37°C water bath for 30 min before being used to treat the cell lines. The cell lines were first treated with increasing concentrations (0, 100, 200, 300, 400 and 500 µM) of PA (Merck, USA), OA (Nacalai Tesque, Japan) and LA (Merck, USA) to determine the cytotoxicity of various FAs. The untreated (0 µM) was treated with MEM or DMEM with 1% BSA. After that, different concentrations were used for different assays as described in the following sections.

2.2 MTT cell proliferation assay

SH-SY5Y,/SH-SY5Y-γ (1.2×10^4 cells/well) or T98G (8×10^3 cells/well) cells were seeded into 96-well plates, treated with different treatment paradigms and incubated for 24 or 48 h. Medium with vehicle (BSA) was used as blank. Then, 20 µl of 5 mg/ml 3-(4,5-dimethylthiazol-2-yl)-2,5-diphenyltetrazolium bromide (MTT, Bio Basic Inc., Canada) prepared in PBS, was added to each well and the plate was incubated at 37 °C for 4 h. The medium in each well was then discarded and 100 µl of DMSO was added into each well. The plate was incubated at 37°C for 30 min prior to absorbance reading at 560 nm using FLUOstar® Omega Microplate Reader (BMG LABTECH, Germany).

2.3 ORO staining of intracellular lipid droplets

After fixation with paraformaldehyde (Sigma-Aldrich, MO, USA) for 1 h, the cells were rinsed with PBS and then stained with freshly diluted ORO solution [3 parts 0.5 % ORO (R&M Chemicals, UK) in isopropyl alcohol and 2 parts of water] for 30 min. The cells were then rinsed twice with water and visualized and photographed using an inverted phase contrast microscope (TS100, Nikon Eclipse, Japan) at 200× magnification.

2.4 Cell death mode and cell cycle analyses by flow cytometry

The cell death mode of SH-SY5Y and T98G cell lines induced by PA was determined using flow cytometry. The cells were stained with annexin V and PI using Alexa Fluor® 488 Annexin V/Dead Cell Apoptosis Kit (Thermo Fisher Scientific, CA, USA). The assay was performed according to the manufacturer's protocol. Briefly, the untreated and treated cells were trypsinised, collected and washed with PBS. Then, the cells were pelleted at 800 *g* for 5 min. The cells were

resuspended at the density of 1 × 10^6 cells/ml with 1× annexin-binding buffer. To every 100 µl of cell suspension, 5 µl of Alexa Fluor® 488 annexin V and 1µl of 100 µg/ml PI (prepared by adding 5 µl of 1 mg/ml stock to 45 µl of 1× annexin-binding buffer) were added. The cells were incubated at room temperature for 15 min. After that, 400 µl of 1× annexin-binding buffer was added and the cells were analysed immediately using Attune™ Nxt Flow Cytometer (Thermo Fisher Scientific, CA, USA). The fluorescence emission was measured using the 530/30 nm (BL1) and 695/40 nm (BL3) emission filters with excitation at 488 nm. Data collected were analysed with Attune™ Nxt Software. Compensation was set up using unstained cells, cells stained with Alexa Fluor® 488 annexin V only and cells stained with PI only.

Cell cycle analysis was performed according to Henry et al. (2013) with slight modification. Briefly, untreated and treated cells were harvested and washed with PBS. The cells were then fixed with 1 ml 70 % ethanol at -20 °C for 1 h. After that, the cells were centrifuged at 2500 *g* for 5 min and the supernatant was discarded. The pellet was resuspended with 1 ml phosphate-citrate wash buffer [200 mM Na_2PO_4 (Merck, USA), 100 mM citric acid (Merck, USA)] followed by centrifugation at 2500 *g* for 5 min. The supernatant was discarded and the cell pellet was resuspended in PI staining solution containing 10 µg/ml PI and 100 µg/ml RNase A prepared in PBS. The cells were analysed using the Attune™ Nxt Flow Cytometer with the 695/40nm (BL3) emission filter. The data collected were analysed using Attune™ Nxt Software

2.5 Intracellular ROS quantification by 2',7'-dichlorofluorescin diacetate (DCFH-DA) assay

Intracellular ROS level was detected using the fluorescent probe DCFH-DA (Sigma-Aldrich,

MO). SH-SY5Y or T98G cell line was seeded with phenol red-free complete medium in black 96-well plates overnight, and 20 µl of 150 µM DCFH-DA (to yield a final concentration of 25 µM) prepared in complete medium was added into each well. The cells were incubated at 37 °C for 45 min before the medium was removed from each well. Next, 100 µl of FA treatment was added and the plate was incubated at 37 °C for 6 h. The fluorescent signal was read at Ex485nm/Em535nm using FLUOstar® Omega Microplate Reader (BMG LABTECH, Germany). Untreated, unstained cells were used as blank.

2.6 Quantification of lipid peroxidation using Thiobarbituric Acid Reactive Substances (TBARS) assay

Parameter™ TBARS Assay kit (R&D Systems, MN, USA) was used to quantify lipid peroxidation by measuring TBARS levels, as an indicator of oxidative stress in cells. The assay was performed in SH-SY5Y and T98G cells after PA treatment, according to the manufacturer's protocol. Briefly, cell lysate was prepared by first collecting the cells and washing the cells with cold PBS. Then, the cells were resuspended in deionised water at the density of 1×10^6 cells/ml. The cell suspension was subjected to a total of 3 cycles of 10-second sonication and then freeze/thaw at ≤ -20°C. Then, 300 µl of the cell lysate was subjected to acid treatment with 300 µl of TBARS Acid Reagent provided in the kit. After 15 min of incubation at room temperature, the mixture was centrifuged at ≥ 12 000 *g* for 4 min and the supernatant was retained. Next, 150µl of standards and samples were added into each well of the microplate and 75 µl of TBA Reagent was added. The optical density of each well was pre-read at 532 nm using FLUOstar® Omega Microplate Reader (BMG LABTECH, Germany). Then, the microplate was covered with the adhesive strip provided and was incubated at 45-50 °C for 2-3 h. After incubation, the optical

density was read at 523 nm. The pre-reading was subtracted from the final reading to correct for the samples contribution to the final absorption at 532 nm. The results were calculated according to the manufacturer's instruction. A linear standard curve was plotted and the concentrations of samples were read from the standard curve and were multiplied by the dilution factor 2.

2.7 Statistical Analysis

Quantitative data were presented as mean ± standard error of mean (S.E.M.) from triplicates of three independent experiments, unless otherwise stated. Statistical analysis was performed using Statistical Package for the Social Sciences (SPSS) software (version 23.0). (SPSS Inc., IL). All results were subjected to paired-sample *t*- test. A *p*-value of < 0.05 was considered as statistically significant.

3. Results

3.1 PA, but not OA and LA, is neurotoxic and gliatoxic

Generally, PA induced cytotoxicity towards SH-SY5Y and SH-SY5Y-γ in a time- and dose-dependent manner at high concentrations. Figures 1 A and B show the effect of PA treatment on the cell lines for 24 and 48 h. At 24 h, the percentage of cell viability significantly decreased dramatically at PA concentrations ≥ 300 µM, while at 48 h, PA concentrations ≥ 200 µM. Except at 500 µM, the cell viability of SH-SY5Y-γ was significantly higher at these concentrations (≥ 300 µM at 24 h, ≥ 200 µM at 48 h). The concentrations of 50% cytotoxicity (LC_{50}) for SH-SY5Y and SH-SY5Y-γ were 420 and 440 µM, respectively, at 24 h, and 320 and 380 µM, respectively, at 48 h. At lower concentrations, PA did not cause cytotoxicity but promoted the growth of SH-SY5Y-γ instead at 48h.

The treatment of OA for 24 and 48 h generally increased the cell viability in both SH-SY5Y and SH-SY5Y-γ, as shown in Figures 1C and D. The cell viability increased as a function of OA concentration and reached the peak of ~140% at 400 μM and 300 μM OA for SH-SY5Y and SH-SY5Y-γ, respectively. For the treatment of LA, the cell viability of SH-SY5Y, but not that of SH-SY5Y-γ, was generally increased, as shown in Figures 1E and F. The results indicate that LA promoted the growth of SH-SY5Y but had no effect on SH-SY5Y-γ at concentrations < 300μM and exerted significant decrease in cell viability (8-18%) at ≥ 400 μM at 48h.

Similar with SH-SY5Y cells, PA at lower concentrations (< 200 μM), induced the growth of astrocytic T98G cells, and while at higher concentrations (≥ 200 μM), reduced the cell viability significantly, in a dose-dependent manner (Figure 1G). The LC_{50} of PA in T98G cells was 320 μM. Like in SH-SY5Y cells, OA also increased the cell viability of T98G at concentrations ≥ 200 μM, while LA did not affect the cell viability significantly (Figure 1G).

3.2 Co-treatment of PQ exacerbates neurotoxicity of PA, but leptin did not ameliorate the neurotoxicity of PA

Co-treatment of PQ exacerbates the neurotoxicity of PA in a dose-dependent manner, as illustrated in Figure 1H. At 200 μM PQ, the cell viability decreased to 41.6 ± 1.2% (Figure 1H). As compared to PQ treatment alone, the LC_{50} was determined to be 380 μM (data not shown). Interestingly, pre-treatment of increasing concentrations of leptin for 6 h not only did not rescue the cells from PA neurotoxicity, it further exacerbates PA neurotoxicity at concentrations ≥ 40 μg/ml (Figure 1I).

3.3 FAs accumulate in SH-SY5Y and T98 cells

To investigate whether the effects of the FAs on SH-SY5Y and T98G cells could be attributed to their transport across the plasma membrane and accumulation in the cytoplasm, ORO staining for intracellular lipid droplets was performed after treatment with 300 μM PA, OA or LA for 24 h. As shown in Figure 2, all FAs accumulate in neuronal and astrocytic cells, with the effect more obvious in the latter. Lipid droplet accumulation was most obvious after PA treatment in T98G cells, accompanied by gliatoxic gross morphological changes (cell number reduction and cell shrinkage) in T98G cells (Figure 2), consistent with the earlier cell viability results in Figure 1G. LA treatment showed the least lipid droplet accumulation in both cell lines. Lipid droplet accumulation after OA or LA treatments did not lead to significant changes in the morphology of SH-SY5Y and T98G cells.

3.4 Transient transfection of α-syn and its PD mutants led to modest rescue from the neurotoxicity of PA

To investigate the gene-environment interaction in affecting neurotoxicity and gliatoxicity, SH-SY5Y and T98G cells were transiently transfected with wt, A30P, E46K or A30P α-syn for 48 h before further treated with LC_{50} of PA (320 μM for both SH-SY5Y and T98G cells). Instead of exacerbating the cytotoxic effect of PA, transient overexpression of wt α-syn or its PD mutants (A30P and E46K, but not A53T) modestly (but still significantly) rescued the neurotoxicity of PA in SH-SY5Y cells (Figure 3A) and T98G cells (Figure 3B; except wt α-syn). Furthermore, transient overexpression of wt, A30P or E46K α-syn also modestly increased the viability of SH-SY5Y cells (but not T98G) when subjected to OA treatment (Figure 3A).

Since the discrepancy in the cytotoxic effect of α-syn overexpression might be due to the transfection method used (transient in this study *vs*. stable in Stefanova et al., 2001), we investigated whether the neurotoxicity results of PA in stable SH-SY5Y-γ cells could be replicated by transient transfection of γ-syn in SH-SY5Y and T98G cells. Indeed, transient transfection of γ-syn did not significantly increase the cell viability of SH-SY5Y cells when subjected to either PA treatment (compared with results in Figure 1B). In short, transient transfection of α-syn or γ-syn will have different effects in SH-SY5Y or T98 cells compared with stable transfection.

3.5 PA induces neurotoxicity and gliatoxicity via apoptotic cell death

To investigate the mode of cell death induced by PA in SH-SH5Y and T98G cells, dual staining with Annexin V and PI was performed and cells were analysed by flow cytometry. The results showed that PA at lower concentrations did not induce apoptosis in SH-SY5Y cells (less than 20% cells undergoing apoptosis) and T98G cells (less than 5% cells undergoing apoptosis), but at 300 μM, PA significantly increased the percentage of apoptotic cells to about 2 fold in both cell lines (Figures 4A, B and E). Single staining with PI for cell cycle analysis by flow cytometry also revealed that DNA fragmentation was statistically significant in 200 μM and 300 μM PA treated cell lines for both SH-SY5Y and T98G (Figures 4C, D and F). For SH-SY5Y cells, the increment in the percentage of DNA fragmentation as indicated by the R1 gate was and 1.3-fold (22.56 ± 0.53% to 28.23 ± 0.03%) and 2.6-fold (from 22.56 ± 0.53% to 57.75 ± 0.19%) for 200 μM and 300 μM PA treatments, respectively (Figure 4F). While for T98G, the increment was 1.5-fold (from 6.74 ± 0.17% to 10.26 ± 0.22%) and 4.1-fold (from 6.74 ± 0.17% to 27.66 ±

0.35%) for 200 μM and 300 μM PA treatments, respectively (Figure 4F). These were associated with the decrease in cell percentages in the other cell cycle phases.

3.6 PA induces apoptotic cell death in SH-SY5Y and T98G cells via oxidative stress

To attribute whether apoptotic cell death induction by PA in SH-SY5Y and T98G is caused by oxidative stress, intracellular ROS (H_2O_2) and extent of lipid peroxidation (TBARS level) were assessed. PA and OA treatments both increased ROS levels in a dose-dependent manner in both SH-SY5Y and T98G cells, with PA induced greater ROS generation as compared to OA (Figure 5). The PA-induced ROS production was at greater extent in T98G (5.39 ± 0.31-fold) as compared to that in SH-SY5Y (2.83 ± 0.16-fold) at 500 μM PA treatment. OA also elevated the level of ROS in both cell lines but to a degree lesser than PA, except 500 μM OA in SH-SY5Y. However, the changes in the lipid peroxidation level were not dose- and time-dependent in both cell lines, as shown in Figure 5. In SH-SY5Y, the level of lipid peroxidation increased 0.3-fold to 1.3-fold at 24 h at 100 and 300 μM PA treatments. At 200 μM, the fold change decreased to 0.5-fold as compared to the untreated. For the 48 h treatment of PA, the level of lipid peroxidation decreased gradually to 0.7-fold of the untreated at 100 and 200 μM, and to 0.5-fold at 300 μM. In T98G, 24 h treatment of PA increased the level of lipid peroxidation to 1.5- and 1.4- fold at 100 and 300 μM, respectively, as compared to the untreated. 200 μM PA decreased the level to 0.8-fold. At 48h, PA treatment on the cell line increased the lipid peroxidation level to 1.3-, 1.1- and 1.8-fold of that of the untreated at 100, 200 and 300 μM, respectively. In short, 300 μM of PA treatment impacted the lipid peroxidation level the most. The changes of lipid peroxidation level in SH-SY5Y were lesser as compared to that of T98G, in which the latter fold change was increased to 1.9-fold at 300 μM after 48h of PA treatment.

4. Discussion

MTT assay results revealed that only PA, but not OA and LA is cytotoxic to all of the three cell lines namely, SH-SY5Y, SH-SY5Y-γ and T98G. The range of FA concentrations used was within the physiological range of circulating free FAs in human plasma, which is ~0.1-1.0 mM (Yuan et al., 2013). The rate of PA β-oxidation was also found to increase as a function of PA concentration, from 15 μM to 2 mM, and peaked at 200 μM, in homogenates of astrocytes cultured from neonatal mouse brain (Murphy et al., 1992). The similar range of FA concentrations had been used in many studies (Gupta et al., 2012; Yuan et al., 2013; Hsiao et al., 2014). The cytotoxic effect of PA observed was similar to that reported earlier. For instance, dose- and time-dependent apoptotic effects were observed in SH-SY5Y after PA treatment. Further elucidation of pathways leading to PA-induced apoptosis revealed that ER stress, as indicated by the expression of spliced X-box binding protein 1 (XBP-1) mRNA and immunoglobin heavy chain-binding protein (BiP), was involved (Kim et al., 2011). In addition, PA inactivated AMPK, and re-activation of AMPK by N1-(β-D-Ribofuranosyl)-5-aminoimidazole-4-carboxamide (AICAR), ameliorated PA-induced cytotoxicity with diminished ER stress-mediated apoptosis (Kim et al., 2011). Correspondingly, Hsiao et al. (2014) also showed that PA triggered SH-SY5Y apoptotic cell death via protein palmitoylation, which induced G_2/M cell cycle arrest and ER stress (Hsiao et al., 2014). On the other hand, OA was found to have neurotrophic effect in neuronal cell line and in rat primary cell cultures (Kwon et al., 2014; Bento-Abreu et al., 2007).

The same cytotoxic effect was also observed in the astrocytic cell line, T98G. This PA-induced

cytotoxicity was also reported previously in primary cultured mouse astrocytes (Wang et al., 2012) and rat cortical astrocytes (Wong et al., 2014). Wang et al. (2012) showed that PA-induced apoptosis in primary mouse astrocytes involved the rise in Bax/Bcl-2 ratio and caspase-3 activation. It involved ROS generation and subsequent mitochondrial membrane potential collapse (Wang et al., 2012; Wong et al., 2014). PA was also found to induce inflammatory response in astrocytes via the Toll-like receptor (TLR) 4, by releasing pro-inflammatory cytokines like TNF-α and IL-6 (Gupta et al., 2012). The inflammatory response was also observed with the treatment of other SFAs, namely, LA and stearic acid, but not unsaturated FAs (like OA) (Gupta et al., 2012).

Although PA induced cytotoxicity in both SH-SY5Y and SH-SY5Y-γ, it was found that PA induced cytotoxicity to a lesser extent in the latter, as indicated by the higher LC_{50}. As a marker of cancer progression, overexpression of γ-syn in ovarian cancer cell lines, A2780 and OVCAR5, was found to enhance tumorigenicity by constitutively activating ERK1/2 and down-regulating JNK1 in response to a host of environmental stress signals (Pan et al., 2002). In human breast cancer cell lines T47D and SKBR3, knockdown of γ-syn sensitized the cells to ER stress-induced apoptosis dependent on JNK or caspase-3 and caspase-7 activation (Hua et al., 2009). Consistent with these, our study suggests an anti-apoptotic role of γ-syn in response to PA-induced cytotoxicity, since the two cells lines used are cancer cell lines.

α-syn and γ-syn, except A53T α-syn, generally increased the cell viability of both SH-SY5Y and T98G cells after PA treatment. Previously, Da Costa et al. (2000) reported that wt α-syn, but not A53T, had anti-apoptotic effect against staurosporine, etoposide and ceramide C in murine

neuronal cell line TSM1. Similarly, our group reported that only wt α-syn, but not the mutant variants, protected SH-SY5Y from the toxicity of rotenone and maneb (Parkinsonian pesticides), by attenuating mitochondrial membrane potential changes and ROS level (Choong & Say, 2011). On the other hand, overexpression of α-syn led to oxidative stress-mediated apoptotic death in U373 astrocytoma cells (Stefanova et al., 2001). In this study, we found that transient overexpression of not only wt, but also A30P, E46K α-syn and γ-syn, were able to ameliorate (albeit modestly) PA-induced cytotoxicity in SH-SY5Y and T98G cells. The discrepancy in the cytotoxic effect of α-syn overexpression might be due to the transfection method used (transient in this study *vs*. stable in Stefanova et al., 2001). A further confirmatory study involving stable overexpression of α-syn and its PD mutants in SH-SY5Y and T98G cells is needed to further elucidate whether α-syn protects against PA-induced cytotoxicity, since α-syn has been shown to bind to the surface of triglyceride-rich lipid droplets and protects them from hydrolysis in cultured cells as well as in primary neurons (Cole et al., 2002).

The co-treatment of PA and PQ brought about intensified cytotoxicity in SH-SY5Y cells as compared to PA or PQ treatment alone. There is no previous study reporting on the interaction between PA and PQ in dopaminergic neurotoxicity, but rotenone, another Parkinsonian environmental toxin which inhibits mitochondrial complex I, was found to increase the incorporation of radioactively-labeled PA into acetyl coA by β-oxidation in SH-SY5Y cells (Worth et al., 2014). In bovine cerebral mitochondria, PQ was reduced to the PQ radical via complex I in mitochondria, leading to accelerated lipid peroxidation, an effect similar to that triggered by rotenone (Fukushima et al., 1995). It is predicted that the PQ-induced lipid peroxidation is further enhanced by PA, which serves as a substrate for CPT-1-dependent

mitochondrial β-oxidation, a process that leads to enhanced ROS production (Magtanong et al., 2016). In addition, PA treatment also triggers the MAPK- and caspase-dependent signaling pathways leading to apoptosis in neuronal N2a cells (Kwon et al., 2014). PQ was found to trigger SH-SY5Y neuronal cell apoptosis via the intrinsic mitochondrial pathway by the upregulation of p53 protein and subsequently, its target pro-apoptotic Bax protein (Yang and Tiffany-Castiglioni, 2008). The impairment of mitochondria complex I activity was followed by the release of cytochrome *c*, increased caspases 9 and 3 activities, nuclear condensation and DNA fragmentation (Yang & Tiffany-Castiglioni, 2008). Thus, it is suggested that PQ and PA synergistically enhance SH-SY5Y cytotoxicity.

Leptin, secreted primarily by adipocytes, is transported across the blood-brain barrier (BBB) and acts on the leptin receptors in the CNS to regulate food intake by modulating the activity of appetite control neurons in the brain (Zhang et al., 1994). Obesity is associated with leptin resistance, where high plasma leptin concentration was observed in most obese humans and rodents but this hyperleptinemia may not reduce appetite or increase energy expenditure (Frederich, Hamann, et al., 1995; Considine et al., 1996). It was reported that leptin receptors, the long and the short isoforms, are expressed in SH-SY5Y (Russo et al., 2004). However, in this study, pre-treatment of leptin was found to exert no cytoprotectivity against PA-induced cell death in SH-SY5Y cells. In a previous study, leptin was found to stimulate cell proliferation in a dose- and time-dependent manner involving the mechanism of apoptosis suppression in SH-SY5Y cells (Russo et al., 2004). SFAs (including PA) were shown to induce ER stress and inflammatory response via toll-like receptor 4 (TLR4) signalling, leading to leptin resistance in rat hypothalamus, whereas rats fed with MUFAs (including OA) did not develop hypothalamic

leptin resistance (Milanski et al., 2009). Therefore, the result suggests a PA-induced leptin resistance in neurons, diminishing its neuroprotective effect.

ORO staining was performed at 24 h time point as there would be too much cell lost in PA treatment after 48 h, in which the cells would appear too sparse in microscopic photographs. FA accumulation was more obvious in astrocytic T98G cell line. This was in-line with published data showing that peripherally administered FAs accumulated primarily in astrocytes, as assayed by radioactivity (Morand et al., 1979; Bernoud et al., 1998). This may be attributed to the FA utilisation in neurons and astrocyte. Edmond et al. (1987) reported that among neurons, astrocytes and oligodendrocytes, only astrocytes were able to utilise FFAs for β-oxidation. Besides, as reviewed by Schönfeld and Reiser (2013), it is speculated that the enzymatic activity of FA oxidation in neuronal mitochondria has been eliminated by evolution as low enzymatic capacity for FA degradation in neural cells was observed. As ATP generation by FA β-oxidation requires more oxygen than glucose, it increases the risk of neurons to become hypoxic (Schönfeld & Reiser, 2013)

The apoptotic cell death was confirmed with flow cytometric analysis using annexin V/PI fluorescent staining and cell cycle analysis. The results are consistent with previous studies (Wang et al., 2012; Hsiao et al., 2014). In SH-SY5Y, PA induced neuron cell cycle G_2/M arrest at 24 h and increased in sub-G_0 phase at 48 h (Hsiao et al., 2014). However, the percentage of apoptotic cells in T98G as quantified by flow cytometry was much lower than that in SH-SY5Y, despite the similar LC_{50} obtained from the MTT assay. This indicates that the use of MTT assay has a limitation, as its rate of tetrazolium reduction may reflect the general metabolic activity or

the rate of glycolytic NADH production, and not the cell number (Berridge et al., 2005). The lesser PA-induced apoptotic cells observed in astrocytic T98G as compared to neuronal SH-SY5Y cells was not in the odd, owing to the high FA β-oxidation rate in astrocytes, as compared to the poor utilisation of FA as fuel in neurons, as discussed earlier (Schönfeld & Reiser, 2013).

In both cell lines, PA and OA treatments were shown to induce ROS generation in a dose-dependent manner in both cell lines. However, the increase in ROS level was found to be higher in T98G than in SH-SY5Y. Also, the degree of lipid peroxidation was higher in T98G cells as compared to that in SH-SY5Y cells. However, there is a similar pattern of increment at 100 μM PA, decrement at 200 μM and rise again at 300 μM in both cell lines, except for the 48h treatment in SH-SY5Y. At 48 h, the fold change in lipid peroxidation degree gradually decreased with increasing PA concentrations in SH-SY5Y. These observations may be attributed by the high FA β-oxidation rate in astrocytes, a most prominent source of ROS generation (Seifert et al., 2010; Rodrigues and Gomes, 2012). β-oxidation of PA yields 15 molecules of flavin adenine dinucleotide ($FADH_2$) and 31 molecules of nicotinamide adenine dinucleotide (NADH) ($FADH_2$/NADH ratio ≈ 0.5) as compared to that of glucose degradation in which 2 molecules of $FADH_2$ and 10 molecules of NADH are generated ($FADH_2$/NADH ratio = 0.2) (Schönfeld & Reiser, 2013). Enhanced ROS generation is observed during the oxidation of $FADH_2$ for ATP generation by the electron transfer flavoprotein-ubiquinone oxidoreductase. Thus, the higher $FADH_2$/NADH ratio of PA β-oxidation in astrocytes would result in elevated ROS level. On the other hand, OA treatment in both cell lines was also shown to increase the ROS level, despite no cytotoxicity effect was detected by MTT assay. This is not unexpected, as OA was found to induce the production of ROS in rat aortic smooth muscle cells (Lu et al., 1998), human

neutrophil (Carrillo et al., 2011) and cultured endothelial cells (bEnd.3) (Gremmels et al., 2015).

5. Conclusions

In summary, PA, but not OA and LA, induced cytotoxicity in SH-SY5Y, SH-SY5Y-γ and T98G cell lines in a time- and dose-dependent manner. The PA-induced cytotoxicity was found to be lower in SH-SY5Y-γ, suggesting its possible role in neuroprotection. Co-treatment of PA and PQ revealed that the PA-induced cytotoxicity was exacerbated by PQ. Leptin did not protect SH-SY5Y cell line from PA-induced neurotoxicity, suggesting a PA-induced leptin resistance. Annexin V/PI and sub-G_0 cell cycle analysis by flow cytometry revealed that PA-induced apoptotic cell death in both SH-SY5Y and T98G cell lines, but the percentage of apoptosis was much lower in T98G with similar concentrations of PA treatment. This indicates that neurons are more susceptible to PA-induced cytotoxicity. The PA-induced apoptotic cell death was found to be associated with increased lipid peroxidation and ROS generation. Taken together, the results suggest that HFD may cause neuronal and astrocytic damage, which indirectly proposes that CNS pathologies involving neuroinflammation and reactive gliosis could be prevented via the diet regimen. Apart from that, the signalling pathways involved in PA-induced apoptotic cell death and the neuroprotection of γ-syn warrant further investigation.

6. References

Argente-arizón P, Freire-regatillo A, Argente J, Chowen JA. (2015). Role of non-neuronal cells in body weight and appetite control. Front Endocrinol (Lausanne). 6:42.

Avila Rodriguez M, Garcia-Segura LM, Cabezas R, Torrente D, Capani F, Gonzalez J, Barreto GE. (2014). Tibolone protects T98G cells from glucose deprivation. J Steroid Biochem

Mol Biol. 144(Pt B):294–303.

Avila-Rodriguez M, Garcia-Segura LM, Hidalgo-Lanussa O, Baez E, Gonzalez J, Barreto GE. (2016). Tibolone protects astrocytic cells from glucose deprivation through a mechanism involving estrogen receptor beta and the upregulation of neuroglobin expression. Mol Cell Endocrinol. 433:35–46.

Bento-Abreu A, Tabernero A, Medina JM. (2007). Peroxisome proliferator-activated receptor-alpha is required for the neurotrophic effect of oleic acid in neurons. J Neurochem. 103:871–81.

Bernoud N, Fenart L, Bénistant C, Pageaux JF, Dehouck MP, Molière P, Lagarde M, Cecchelli R, Lecerf J. (1998). Astrocytes are mainly responsible for the polyunsaturated fatty acid enrichment in blood-brain barrier endothelial cells in vitro. J Lipid Res. 39:1816-24.

Berridge MV, Herst PM, Tan AS. (2005). Tetrazolium dyes as tools in cell biology: new insights into their cellular reduction. Biotechnol Annu Rev. 11:127–52.

Braak H, Sastre M, Del Tredici K. (2007). Development of alpha-synuclein immunoreactive astrocytes in the forebrain parallels stages of intraneuronal pathology in sporadic Parkinson's disease. Acta Neuropathol. 114:231–41.

Buckman LB, Thompson MM, Moreno HN, Ellacott KL. (2013). Regional astrogliosis in the mouse hypothalamus in response to obesity. J Comp Neurol. 521(6):1322-33.

Cabezas R, Avila MF, Gonzalez J, El-Bacha RS, Barreto GE. (2015). PDGF-BB protects mitochondria from rotenone in T98G cells. Neurotox Res. 27:355–367.

Carrillo, C. Del Mar Cavia M, Roelofs H, Wanten G, Alonso-Torre SR. (2011). Activation of human neutrophils by oleic acid involves the production of reactive oxygen species and a rise in cytosolic calcium concentration: a comparison with N-6 polyunsaturated fatty

acids. Cell Physiol Biochem. 28:329–38.

Choong CJ, Say YH. (2011). Neuroprotection of alpha-synuclein under acute and chronic rotenone and maneb treatment is abolished by its familial Parkinson's disease mutations A30P, A53T and E46K. NeuroToxicol. 32:857–63.

Cole NB, Murphy DD, Grider T, Rueter S, Brasaemle D, Nussbaum RL. (2002). Lipid droplet binding and oligomerization properties of the Parkinson's disease protein α-synuclein. J Biol Chem. 277:6344–52.

Considine RV, Sinha MK, Heiman ML, Kriauciunas A, Stephens TW, Nyce MR, Ohannesian JP, Marco CC, McKee LJ, Bauer TL, Caro JF. (1996). Serum immunoreactive-leptin concentrations in normal-weight and obese humans. N Engl J Med. 334:292–5.

Da Costa CA, Ancolio K, Checler F. (2000). Wild-type but not Parkinson's disease-related Ala-53 → Thr mutant α-Synuclein protects neuronal cells from apoptotic stimuli. J Biol Chem. 275:24065–9.

Dorfman MD, Thaler JP. (2015). Hypothalamic inflammation and gliosis in obesity. Curr Opin Endocrinol Diabetes Obes. 22:325-30.

Edmond J, Robbins RA, Bergstrom JD, Cole RA, de Vellis J. (1987). Capacity for substrate utilization in oxidative metabolism by neurons, astrocytes, and oligodendrocytes from developing brain in primary culture. J Neurosci Res. 1987;18:551-61.

Fabelo N, Martín V, Santpere G, Marín R, Torrent L, Ferrer I, Díaz M. (2011). Severe alterations in lipid composition of frontal cortex lipid rafts from Parkinson's disease and incidental Parkinson's disease. Mol Med. 17:1107–18.

Fraser T, Tayler H, Love S. (2010). Fatty acid composition of frontal, temporal and parietal neocortex in the normal human brain and in Alzheimer's disease. Neurochem Res.

35:503–13.

Frederich RC, Hamann A, Anderson S, Löllmann B, Lowell BB, Flier JS. (1995). Leptin levels reflect body lipid-content in mice: evidence for diet-induced resistance to leptin action. Nat Med. 1:1311-4.

Freire-Regatillo A, Argente-Arizón P, Argente J, García-Segura LM, Chowen JA. (2017). Non-neuronal cells in the hypothalamic adaptation to metabolic signals. Front Endocrinol (Lausanne). 8:51.

Fukushima T, Tawara T, Isobe A, Hojo N, Shiwaku K, Yamane Y. 1995. Radical formation site of cerebral complex I and Parkinson's disease. J Neurosci Res. 42:385-90.

Golovko MY, Faergeman NJ, Cole NB, Castagnet PI, Nussbaum RL, Murphy EJ. (2005). α-synuclein gene deletion decreases brain palmitate uptake and alters the palmitate metabolism in the absence of a-synuclein palmitate binding. Biochemistry. 44:8251–9.

Gremmels H, Bevers LM, Fledderus JO, Braam B, van Zonneveld AJ, Verhaar MC, Joles JA. (2015). Oleic acid increases mitochondrial reactive oxygen species production and decreases endothelial nitric oxide synthase activity in cultured endothelial cells. Eur J Pharmacol. 751:67-72.

Guest J, Garg M, Bilgin A, Grant, R. (2013). Relationship between central and peripheral fatty acids in humans. Lipids Health Dis. 12:79.

Guillemot-Legris O, Muccioli GG. (2017). Obesity-induced neuroinflammation: beyond the hypothalamus. Trends in Neurosci. 40:237–53.

Gunstone FD, Harwood JL, Dijkstra AJ. (2010). The lipid handbook with CD-ROM. CRC Press: Boca Raton, FL, USA.

Gupta S, Knight AG, Gupta S, Keller JN, Bruce-Keller AJ. (2012). Saturated long-chain fatty

acids activate inflammatory signaling in astrocytes. J Neurochem. 120:1060-71.

Gustafson D, Rothenberg E, Blennow K, Steen B, Skoog I. (2003). An 18-year follow-up of overweight and risk of Alzheimer disease. Arch Intern Med. 163:1524-8.

Henry CM, Hollville E, Martin SJ (2013). Measuring apoptosis by microscopy and flow cytometry. Methods. 61:90–7.

Hsiao J-H, Halliday GM, Kim WS. (2017). α-synuclein regulates neuronal cholesterol efflux. Molecules. 22:1769.

Hsiao YH, Lin CI, Liao H, Chen YH, Lin SH. (2014). Palmitic acid-induced neuron cell cycle G2/M arrest and endoplasmic reticular stress through protein palmitoylation in SH-SY5Y human neuroblastoma cells. Int J Mol Sci.15:20876-99.

Hu G, Jousilahti P, Nissinen A, Antikainen R, Kivipelto M, Tuomilehto J. (2006). Body mass index and the risk of Parkinson disease. Neurology. 67:1955–9.

Hua H, Xu L, Wang J, Jing J, Luo T, Jiang Y. (2009). Up-regulation of gamma-synuclein contributes to cancer cell survival under endoplasmic reticulum stress. J Pathol. 217:507–515.

Karmi A, Iozzo P, Viljanen A, Hirvonen J, Fielding BA, Virtanen K, Oikonen V, Kemppainen J, Viljanen T, Guiducci L, Haaparanta-Solin M, Någren K, Solin O, Nuutila P. (2010). Increased brain fatty acid uptake in metabolic syndrome. Diabetes. 59:2171–7.

Kim J, Park Y-J, Jang Y, Kwon YH. (2011). AMPK activation inhibits apoptosis and tau hyperphosphorylation mediated by palmitate in SH-SY5Y cells. Brain Res. 1418:42–51.

Kwon B, Lee H-K, Querfurth HW. (2014). Oleate prevents palmitate-induced mitochondrial dysfunction, insulin resistance and inflammatory signaling in neuronal cells. Biochim Biophys Acta. 1843:1402–13.

Logroscino G, Marder K, Cote L, Tang MX, Shea S, Mayeux R. (1996). Dietary lipids and antioxidants in Parkinson's disease: a population-based, case-control study. Ann Neurol. 39:89-94.

Lu G, Greene EL, Nagai T, Egan BM. (1998). Reactive oxygen species are critical in the oleic acid-mediated mitogenic signaling pathway in vascular smooth muscle cells. Hypertension. 32:1003–10.

Lu J, Park CS, Lee SK, Shin DW, Kang JH. (2006). Leptin inhibits 1-methyl-4-phenylpyridinium-induced cell death in SH-SY5Y cells. Neurosci Lett. 407:240–3.

Magtanong L, Ko PJ, Dixon SJ. (2016). Emerging roles for lipids in non-apoptotic cell death. Cell Death Diff. 23:1099–109.

Milanski M, Degasperi G, Coope A, Morari J, Denis R, Cintra DE, Tsukumo DM, Anhe G, Amaral ME, Takahashi HK, Curi R, Oliveira HC, Carvalheira JB, Bordin S, Saad MJ, Velloso LA. (2009). Saturated fatty acids produce an inflammatory response predominantly through the activation of TLR4 signaling in hypothalamus: implications for the pathogenesis of obesity. J Neurosci. 29:359-70.

Millership S, Ninkina N, Rochford JJ, Buchman VL. (2013). γ-synuclein is a novel player in the control of body lipid metabolism. Adipocyte 2:276–80.

Morand O, Baumann N, Bourre JM. (1979). In vivo incorporation of exogenous [1-14C] stearic acid into neurons and astrocytes. Neurosci Lett. 13:177–81.

Murphy MG, Jollimore C, Crocker JFS, Her H. (1992). B-Oxidation of [114C]palmitic acid by mouse astrocytes in primary culture: effects of agents implicated in the encephalopathy of Reye's syndrome. J. Neurosci. Res. 33:445–54.

Pan ZZ, Bruening W, Giasson BI, Lee VM-Y, Godwin AK.. (2002). γ-synuclein promotes

cancer cell survival and inhibits stress- and chemotherapy drug-induced apoptosis by modulating MAPK pathways. J Biol Chem. 277:35050–60.

Park HR, Kim J-Y, Park K-Y, Lee J. (2011). Lipotoxicity of palmitic acid on neural progenitor cells and hippocampal neurogenesis. Toxicol Res. 27:103–10.

Pezzoli G, Cereda E. (2013). Exposure to pesticides or solvents and risk of Parkinson disease. Neurology 80:2035–41.

Polymeropoulos MH, Lavedan C, Leroy E, Ide SE, Dehejia A, Dutra A, Pike B, Root H, Rubenstein J, Boyer R, Stenroos ES, Chandrasekharappa S, Athanassiadou A, Papapetropoulos T, Johnson WG, Lazzarini AM, Duvoisin RC, Di Iorio G, Golbe LI, Nussbaum RL. (1997). Mutation in the α-synuclein gene identified in families with Parkinson's disease. Science. 276:2045–7.

Rodrigues JV, Gomes CM. (2012). Mechanism of superoxide and hydrogen peroxide generation by human electron-transfer flavoprotein and pathological variants. Free Radic Biol Med. 53:12–9.

Russo VC, Metaxas S, Kobayashi K, Harris M, Werther GA. (2004). Antiapoptotic effects of leptin in human neuroblastoma cells. Endocrinology. 145:4103–12.

Sääksjärvi K, Knekt P, Männistö S, Lyytinen J, Jääskeläinen T, Kanerva N, Heliövaara M. (2014). Reduced risk of Parkinson's disease associated with lower body mass index and heavy leisure-time physical activity. Eur J Epidemiol. 29:285-92.

Schönfeld P, Reiser G. (2013). Why does brain metabolism not favor burning of fatty acids to provide energy? - Reflections on disadvantages of the use of free fatty acids as fuel for brain. J Cereb Blood Flow Metab. 33:1493-9.

Seifert EL, Estey C, Xuan JY, Harper ME. (2010). Electron transport chain-dependent and -

independent mechanisms of mitochondrial H2O2 emission during long-chain fatty acid oxidation. J Biol Chem. 285:5748–58.

Spillantini MG, Goedert M. (2000). The alpha-synucleinopathies: Parkinson's disease, dementia with Lewy bodies, and multiple system atrophy. Ann N Y Acad Sci. 920:16–27.

Stefanova N, Klimaschewski L, Poewe W, Wenning GK, Reindl M. (2001). Glial cell death induced by overexpression of alpha-synuclein. J Neurosci Res. 65:432–8.

Wakabayashi K, Hayashi S, Yoshimoto M, Kudo H, Takahashi H. (2000). NACP/alpha-synuclein-positive filamentous inclusions in astrocytes and oligodendrocytes of Parkinson's disease brains. Acta Neuropathol. 99:14–20.

Wang Z, Liu D, Wang J, Liu S, Gao M, Ling EA, Hao A. (2012). Cytoprotective effects of melatonin on astroglial cells subjected to palmitic acid treatment in vitro. J Pineal Res. 52:253-64.

Weng Z, Signore AP, Gao Y, Wang S, Zhang F, Hastings T, Yin XM, Chen J. (2007). Leptin protects against 6-hydroxydopamine-induced dopaminergic cell death via mitogen-activated protein kinase signaling. J Biol Chem. 282:34479-91.

Wong KL, Wu YR, Cheng KS, Chan P, Cheung CW, Lu DY, Su TH, Liu ZM, Leung YM. (2014). Palmitic acid-induced lipotoxicity and protection by (+)-catechin in rat cortical astrocytes. Pharmacol Rep. 66:1106–13.

World Health Organization. (2018). Obesity and overweight [Online]. Available at: http://www.who.int/mediacentre/factsheets/fs311/en/ [Accessed: 26 February 2018].

Worth AJ, Basu SS, Snyder NW, Mesaros C, Blair IA. (2014). Inhibition of neuronal cell mitochondrial complex i with rotenone increases lipid β-oxidation, supporting acetyl-coenzyme a levels. J Biol Chem. 289:26895-903.

Xie HR, Hu LS, Li GY. (2010). SH-SY5Y human neuroblastoma cell line: in vitro cell model of dopaminergic neurons in Parkinson's disease. Chin Med J (Engl). 123:1086-92.

Yang W, Tiffany-Castiglioni E. (2008). Paraquat-induced apoptosis in human neuroblastoma SH-SY5Y cells: involvement of p53 and mitochondria. J Toxicol Environ Health A. 71:289-99.

Yuan Q, Zhao S, Wang F, Zhang H, Chen ZJ, Wang J, Wang Z, Du Z, Ling EA, Liu Q, Hao A. (2013). Palmitic acid increases apoptosis of neural stem cells via activating c-Jun N-terminal kinase. Stem Cell Res. 10:257-66.

Zhang L, Ji J, Zhu XY, Wu YY, Yu H, Zhang B, Li XL, Sun XZ. (2004). Palmitic acid induces apoptosis in human hepatoma cell line, HepG2 cells. Zhongguo Yi Xue Ke Xue Yuan Xue Bao. 26:671-6.

Zhang Y, Proenca R, Maffei M, Barone M, Leopold L, Friedman JM. (1994). Positional cloning of the mouse obese gene and its human homologue. Nature. 372:425–32.

Figure legends

Figure 1: PA, but not OA or LA, is neurotoxic and gliatoxic to SH-SY5Y and T98G cells, and the effects are ameliorated by γ-syn overexpression and exacerbated by PQ treatment. SH-SY5Y and SH-SY5Y-γ cells were treated with increasing concentrations of PA (**A**, **B**), OA (**C**, **D**) and LA (**E**, **F**) for 24 h (**A**, **C**, **E**) or 48 h (**B**, **D**, **F**). Data represent mean ± S.E.M. of three independent experiments; a and b represent $p < 0.05$ as compared to the untreated for SH-SY5Y and SH-SY5Y-γ, respectively. **G**. Effects of fatty acid treatments in T98G cell line. T98G cells were treated with increasing concentrations (0, 100, 200, 300, 400 and 500 μM) of PA, OA and LA for 48 h. **H**. SH-SY5Y cells were co-treated with 300 μM PA and with increasing

concentrations (0, 200, 400, 600, and 800 μM) of PQ for 48 h. MTT assay was then performed. Data represent mean ± S.E.M. of three independent experiments; * represents $p < 0.05$ as compared to 300 μM of PA treatment. **I**. SH-SY5Y cells were pre-treated with increasing concentrations (0, 10, 20, 30, 40 and 50 μg/ml) of leptin for 6 h followed by 300 μM PA treatment for 48 h. MTT assay was then performed. Data represent mean ± S.E.M. of three independent experiments; * represents $p < 0.05$ as compared to untreated.

Figure 2: ORO staining of SH-SY5Y and T98G after fatty acid treatments. SH-SY5Y and T98G cells were treated with PA, OA and LA for 24 h followed by ORO staining. The pictures show the morphological changes of the cells captured using NIS-Elements BR 3.0 software under Nikon Eclipse TS100 inverted microscope at 200× magnification.

Figure 3: Effects of PA and OA on α-syn or γ-syn transient-transfected SH-SY5Y and T98G cells. SH-SY5Y and T98G cells were transfected with wild type (WT), different mutants of α-syn (A30P, E46K and A53T) and γ-syn for 48 h followed by the treatment of 300 μM of PA or OA for 48 h. Then, MTT assay was performed. **A**. SH-SY5Y. **B**. T98G. Data represent mean ± S.E.M. of three independent experiments; * represents $p < 0.05$ as compared to the untransfected, untreated.

Figure 4: Annexin V-FITC/PI flow cytometric analysis of apoptosis and cell cycle in SH-SY5Y and T98G cells after 48 h of PA treatment. SH-SY5Y and T98G cells were treated with increasing concentrations (0, 100, 200 and 300 μM) of PA for 48 h. Cells were stained with annexin V-FITC and PI followed by flow cytometric analysis. Representative dot plots from one

experiment are shown. -/+ = necrosis, +/+ = late apoptosis, -/- = live cells and +/- = early apoptosis. **A**. SH-SY5Y. **B**. T98G. Cell cycle distribution was also analysed by flow cytometry. Representative DNA content histograms from one experiment were presented. R1 = Sub-G_0/G_1 phase, R2 = G_0/G_1 phase, R3 = S phase and R4 = G_2/M phase. **C**. SH-SY5Y. **D**. T98G. **E**. Statistical graph of the '+/- quadrant' of the dot plots of SH-SY5Y and T98G cells. Data represent the mean ± S.E.M. of three independent experiments. * represents $p < 0.01$ as compared to untreated. **F.** Statistical graph of R1 gate of SH-SY5Y and T98G cells. Data represent the mean ± S.E.M. of three independent experiments. * represents $p < 0.01$ as compared to untreated.

Figure 5: Measurement of ROS generation and lipid peroxidation in SH-SY5Y and T98G cells after PA and OA treatment. SH-SY5Y and T98G cells were treated with increasing concentrations (0, 100, 200 300, 400 and 500μM) of PA or OA for 6 h and the ROS generation was measured using the DCFH-DA assay. Figure shows the fold change in fluorescent intensity as compared to the untreated group. **A**. SH-SY5Y. **B**. T98G; Data represent the mean ± S.E.M. of three independent experiments; * represents $p < 0.05$ as compared to the untreated. SH-SY5Y and T98G cells were also treated with increasing concentrations (0, 100, 200 and 300 μM) of PA for 24 h or 48 h and TBARS assay was then performed. **C**. SH-SY5Y. **D**. T98G. Data represent the mean ± S.E.M. of three independent experiments; * represents $p < 0.05$ as compared to untreated.

Figure 1

PA, but not OA or LA, is neurotoxic and gliatoxic to SH-SY5Y and T98G cells, and the effects are ameliorated by γ-syn overexpression and exacerbated by PQ treatment

SH-SY5Y and SH-SY5Y-γ cells were treated with increasing concentrations of PA (A, B), OA (C, D) and LA (E, F) for 24 h (A, C, E) or 48 h (B, D, F). Data represent mean ± S.E.M. of three independent experiments; a and b represent $p < 0.05$ as compared to the untreated for SH-SY5Y and SH-SY5Y-γ, respectively. G. Effects of fatty acid treatments in T98G cell line. T98G cells were treated with increasing concentrations (0, 100, 200, 300, 400 and 500 μM) of PA, OA and LA for 48 h. H. SH-SY5Y cells were co-treated with 300 μM PA and with increasing concentrations (0, 200, 400, 600, and 800 μM) of PQ for 48 h. MTT assay was then performed. Data represent mean ± S.E.M. of three independent experiments; * represents $p < 0.05$ as compared to 300 μM of PA treatment. I. SH-SY5Y cells were pre-treated with increasing concentrations (0, 10, 20, 30, 40 and 50 μg/ml) of leptin for 6 h followed by 300 μM PA treatment for 48 h. MTT assay was then performed. Data represent mean ± S.E.M. of three independent experiments; * represents $p < 0.05$ as compared to untreated.

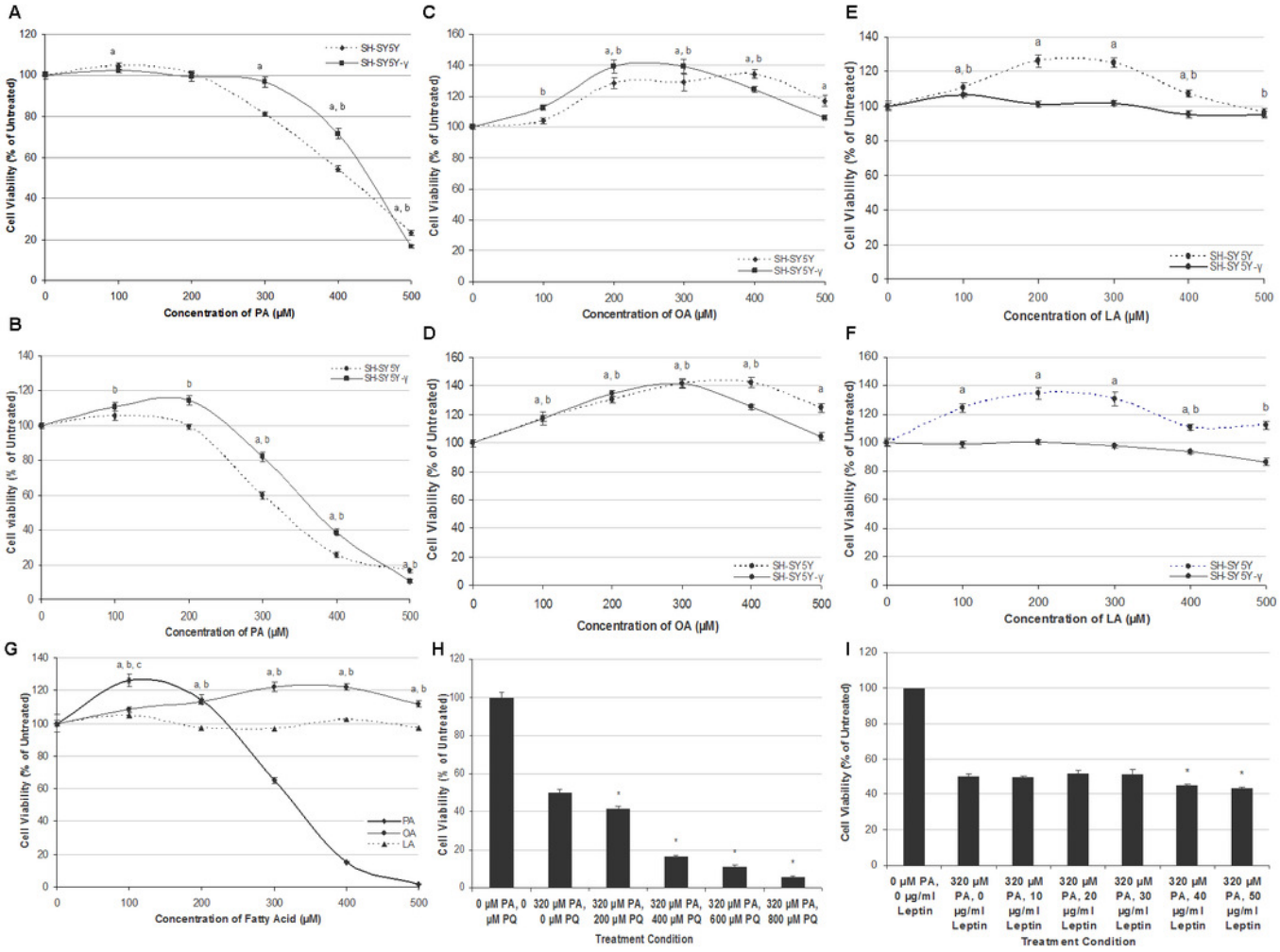
A
Cell Viability (% of Untreated)
Concentration of PA (μM)
SH-SY5Y
SH-SY5Y-γ
B
Cell viability (% of Untreated)
Concentration of PA (μM)
C
Cell Viability (% of Untreated)
Concentration of OA (μM)
D
Cell Viability (% of Untreated)
Concentration of OA (μM)
E
Cell Viability (% of Untreated)
Concentration of LA (μM)
F
Cell Viability (% of Untreated)
Concentration of LA (μM)
G
Cell Viability (% of Untreated)
Concentration of Fatty Acid (μM)
PA
OA
LA
H
Cell Viability (% of Untreated)
0 μM PA, 0 μM PQ
320 μM PA, 0 μM PQ
320 μM PA, 200 μM PQ
320 μM PA, 400 μM PQ
320 μM PA, 600 μM PQ
320 μM PA, 800 μM PQ
Treatment Condition
I
Cell Viability (% of Untreated)
0 μM PA, 0 μg/ml Leptin
320 μM PA, 0 μg/ml Leptin
320 μM PA, 10 μg/ml Leptin
320 μM PA, 20 μg/ml Leptin
320 μM PA, 30 μg/ml Leptin
320 μM PA, 40 μg/ml Leptin
320 μM PA, 50 μg/ml Leptin
Treatment Condition

Figure 2

ORO staining of SH-SY5Y and T98G after fatty acid treatments

SH-SY5Y and T98G cells were treated with PA, OA and LA for 24 h followed by ORO staining. The pictures show the morphological changes of the cells captured using NIS-Elements BR 3.0 software under Nikon Eclipse TS100 inverted microscope at 200× magnification.

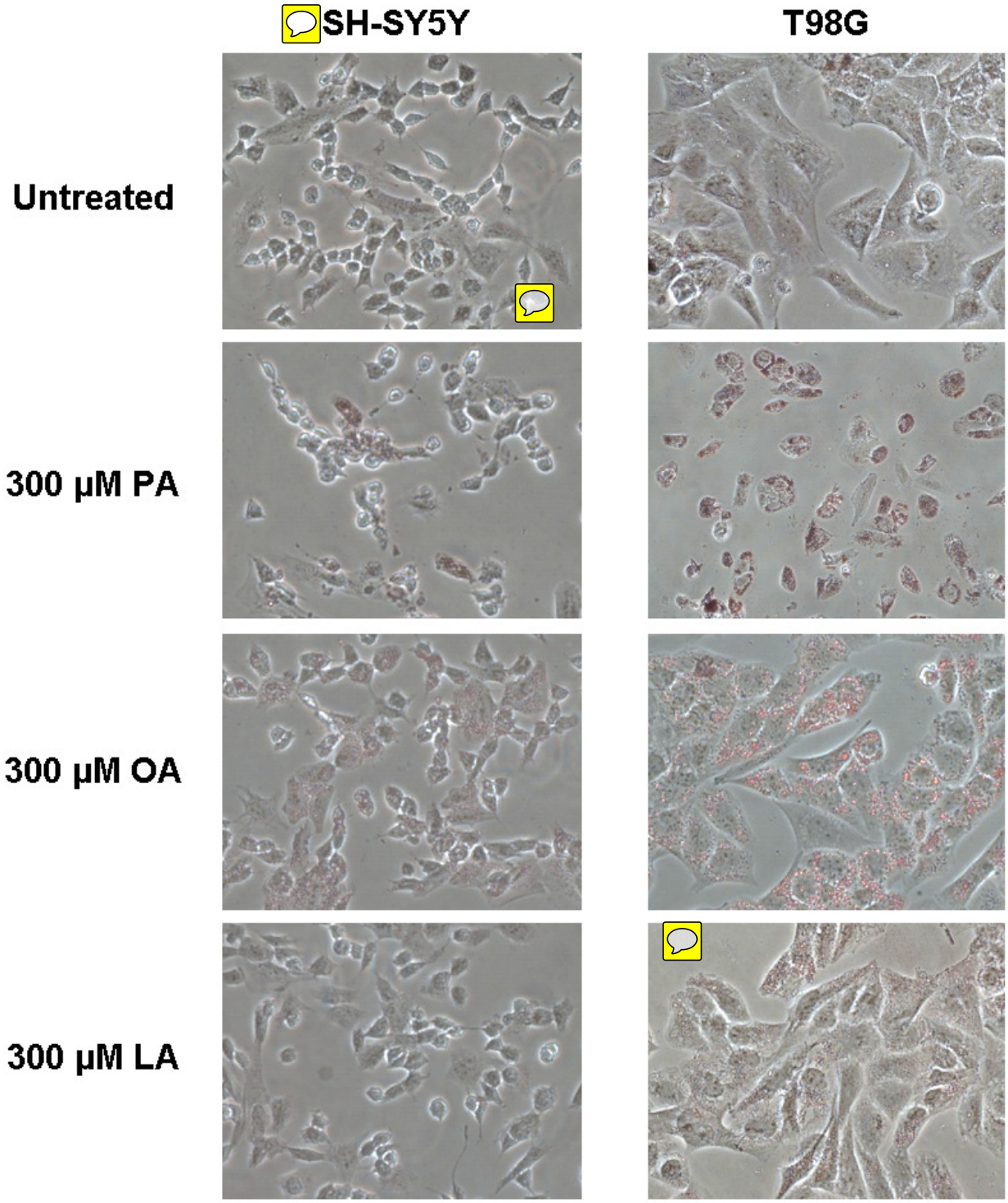
SH-SY5Y
T98G
Untreated
300 µM PA
300 µM OA
300 µM LA

Figure 3

Effects of PA and OA on α-syn or γ-syn transient-transfected SH-SY5Y and T98G cells

SH-SY5Y and T98G cells were transfected with wild type (WT), different mutants of α-syn (A30P, E46K and A53T) and γ-syn for 48 h followed by the treatment of 300 μM of PA or OA for 48 h. Then, MTT assay was performed. A. SH-SY5Y. B. T98G. Data represent mean ± S.E.M. of three independent experiments; * represents $p < 0.05$ as compared to the untransfected, untreated.

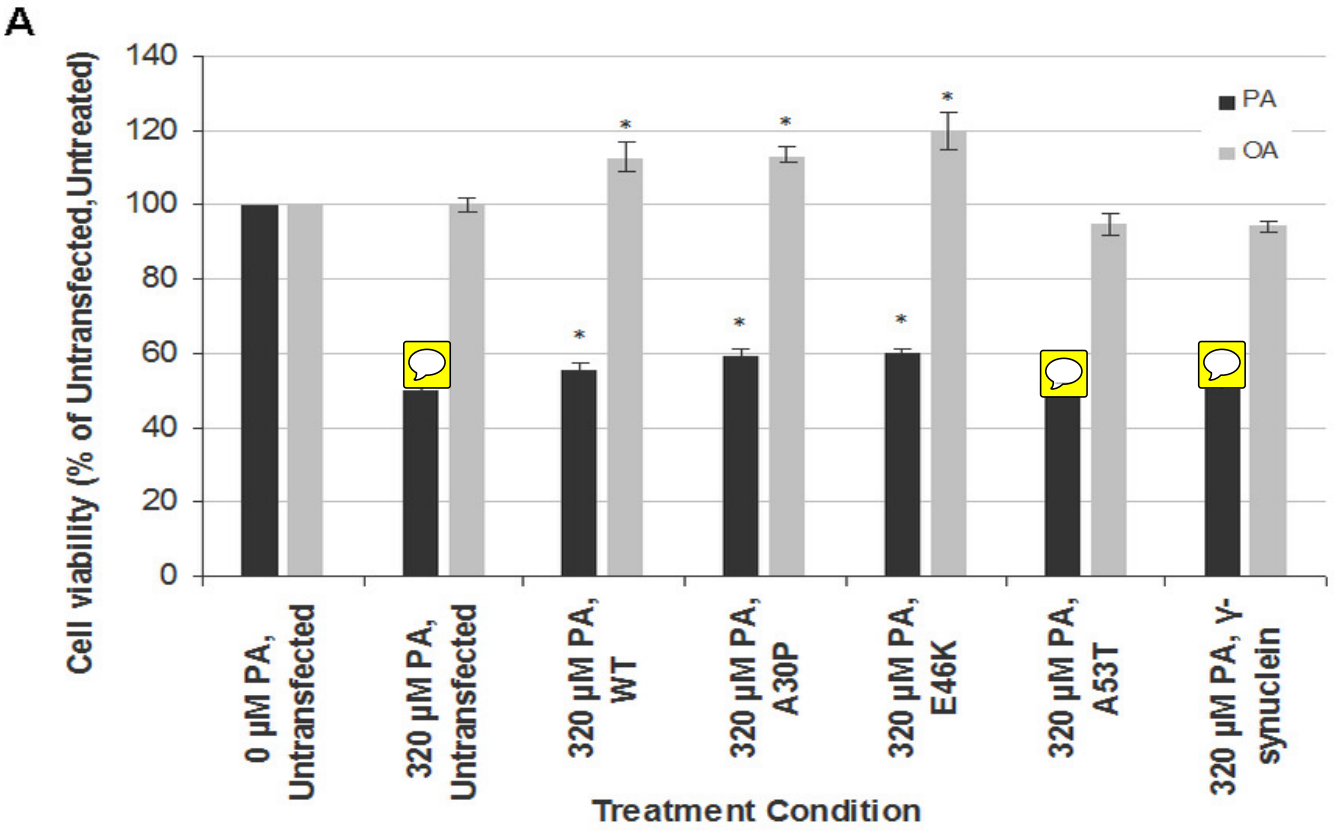
A
Cell viability (% of Untransfected,Untreated)
140
120
100
80
60
40
20
0
PA
OA
0 µM PA, Untransfected
320 µM PA, Untransfected
320 µM PA, WT
320 µM PA, A30P
320 µM PA, E46K
320 µM PA, A53T
320 µM PA, γ-synuclein
Treatment Condition

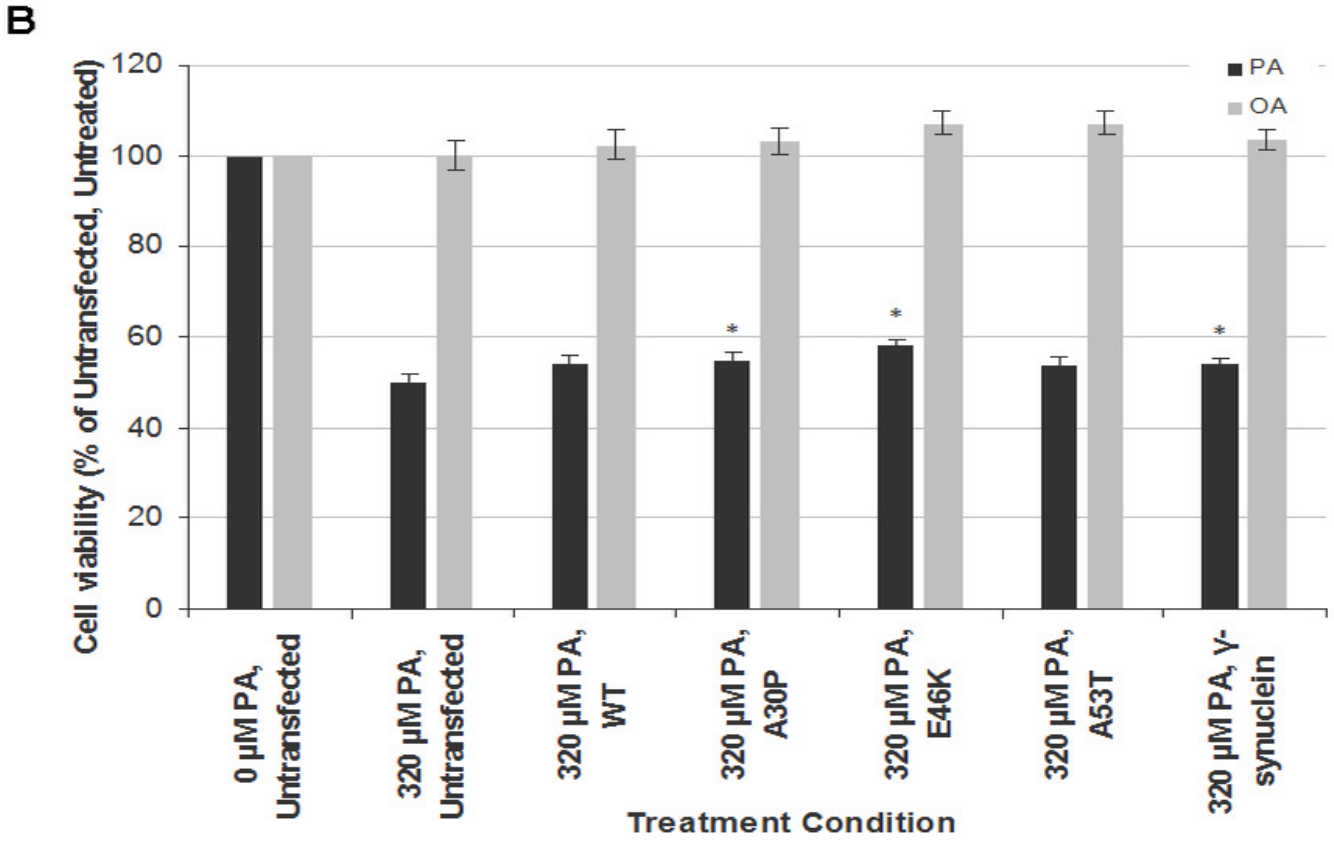
B
Cell viability (% of Untransfected, Untreated)
120
100
80
60
40
20
0
PA
OA
0 µM PA, Untransfected
320 µM PA, Untransfected
320 µM PA, WT
320 µM PA, A30P
320 µM PA, E46K
320 µM PA, A53T
320 µM PA, γ-synuclein
Treatment Condition

Figure 4

~~Annexin V-FITC/PI~~ flow cytometric analysis of apoptosis and cell cycle in SH-SY5Y and T98G cells after 48 h of PA treatment

SH-SY5Y and T98G cells were treated with increasing concentrations (0, 100, 200 and 300 μM) of PA for 48 h. Cells were stained with annexin V-FITC and PI followed by flow cytometric analysis. Representative dot plots from one experiment are shown. -/+ = necrosis, +/+ = late apoptosis, -/- = live cells and +/- = early apoptosis. A. SH-SY5Y. B. T98G. Cell cycle distribution was also analysed by flow cytometry. Representative DNA content histograms from one experiment were presented. R1 = Sub-G¬0/G1 phase, R2 = G0/G¬1 phase, R3 = S phase and R4 = G2/M phase. C. SH-SY5Y. D. T98G. E. Statistical graph of the '+/- quadrant' of the dot plots of SH-SY5Y and T98G cells. Data represent the mean ± S.E.M. of three independent experiments. * represents $p < 0.01$ as compared to untreated. F. Statistical graph of R1 gate of SH-SY5Y and T98G cells. Data represent the mean ± S.E.M. of three independent experiments. * represents $p < 0.01$ as compared to untreated.

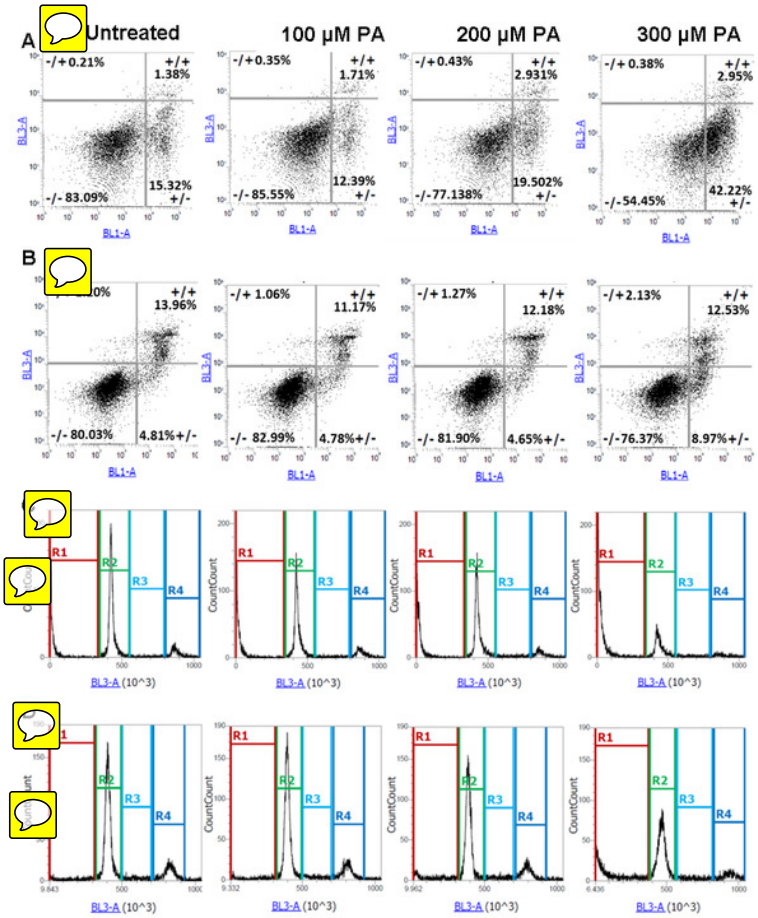
A
Untreated
100 μM PA
200 μM PA
300 μM PA
-/+0.21%
+/+ 1.38%
15.32% +/-
-/- 83.09%
-/+0.35%
+/+ 1.71%
12.39% +/-
-/- 85.55%
-/+0.43%
+/+ 2.931%
19.502% +/-
-/-77.138%
-/+0.38%
+/+ 2.95%
42.22% +/-
-/-54.45%
BL3-A
BL1-A
B
+/+ 13.96%
-/- 80.03%
4.81%+/-
-/+ 1.06%
+/+ 11.17%
-/- 82.99%
4.78%+/-
-/+1.27%
+/+ 12.18%
-/- 81.90%
4.65%+/-
-/+2.13%
+/+ 12.53%
-/-76.37%
8.97%+/-
R1
R2
R3
R4
CountCount
BL3-A (10^3)

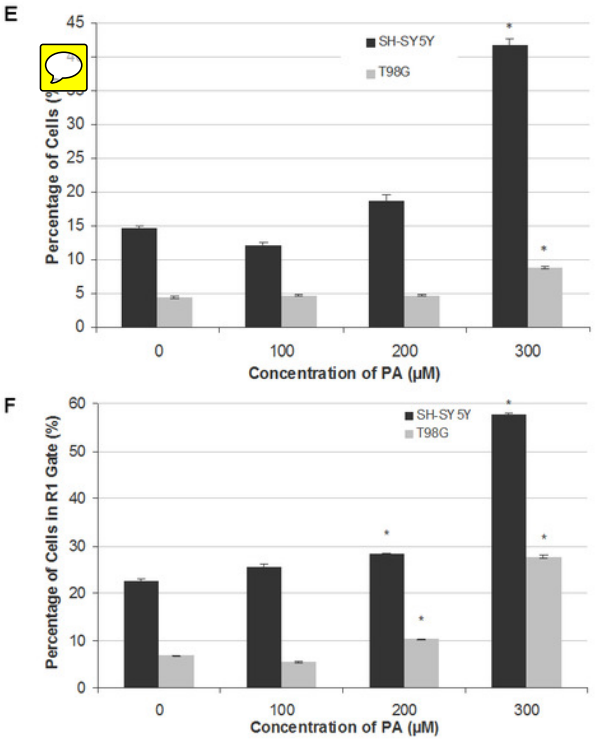
E
SH-SY5Y
T98G
Percentage of Cells (%)
Concentration of PA (μM)
0
100
200
300
F
Percentage of Cells in R1 Gate (%)

Figure 5

Measurement of ROS generation and lipid peroxidation in SH-SY5Y and T98G cells after PA and OA treatment

SH-SY5Y and T98G cells were treated with increasing concentrations (0, 100, 200 300, 400 and 500μM) of PA or OA for 6 h and the ROS generation was measured using the DCFH-DA assay. Figure shows the fold change in fluorescent intensity as compared to the untreated group. A. SH-SY5Y. B. T98G; Data represent the mean ± S.E.M. of three independent experiments; * represents $p < 0.05$ as compared to the untreated. SH-SY5Y and T98G cells were also treated with increasing concentrations (0, 100, 200 and 300 μM) of PA for 24 h or 48 h and TBARS assay was then performed. C. SH-SY5Y. D. T98G. Data represent the mean ± S.E.M. of three independent experiments; * represents $p < 0.05$ as compared to untreated.